Cytokines and metabolites are the main descriptors of severe asthma in children when performing multi-omics analysis of bronchoaleveolar lavages

Mélanie Briard, Blanche Guillon, Eric Venot, Marta Grauso, Christelle Hennequet-Antier, Aurelia Bruneau, François Fenaille, Florence Castelli, Muriel Thomas, Guillaume Lezmi, et al.

▶ **To cite this version:**

HAL Id: hal-04678528
https://hal.inrae.fr/hal-04678528v1

Preprint submitted on 27 Aug 2024

Cytokines and metabolites are the main descriptors of severe asthma in children when performing multi-omics analysis of bronchoaleveolar lavages

Mélanie Briard

Université Paris-Saclay, CEA, INRAE, UMR Département Médicaments et Technologies pour la Santé (DMTS)

Blanche Guillon

Université Paris-Saclay, CEA, INRAE, UMR Département Médicaments et Technologies pour la Santé (DMTS)

Eric Venot

Université Paris-Saclay, CEA, INRAE, UMR Département Médicaments et Technologies pour la Santé (DMTS)

Marta Grauso

Université Paris-Saclay, CEA, INRAE, UMR Département Médicaments et Technologies pour la Santé (DMTS)

Christelle Hennequet-Antier

Université Paris-Saclay, MIGALE Bioinformatics Facility

Aurélia Bruneau

Université Paris-Saclay, INRAE, UMR1319 Micalis Institute

François Fenaille

Université Paris-Saclay, CEA, INRAE, UMR Département Médicaments et Technologies pour la Santé (DMTS)/SPI/Laboratoire innovations en spectrométrie de masse pour la santé

Florence Castelli

Université Paris-Saclay, CEA, INRAE, UMR Département Médicaments et Technologies pour la Santé (DMTS)/SPI/Laboratoire innovations en spectrométrie de masse pour la santé

Muriel Thomas

Université Paris-Saclay, INRAE, UMR1319 Micalis Institute

Guillaume Lezmi

AP-HP, Hôpital Necker-Enfants Malades

Maria Leite-de-Moraes

Université de Paris Cité, Institut Necker Enfants Malades, Inserm UMR1151, CNRS UMR8253

Vinciane Saint-Criq (✉ vinciane.saint-criq@inrae.fr)

Université Paris-Saclay, INRAE, UMR1319 Micalis Institute

Karine Adel-Patient

Université Paris-Saclay, CEA, INRAE, UMR Département Médicaments et Technologies pour la Santé (DMTS)

Research Article

Abstract

Background. Severe asthma (SA) is a heterogeneous condition with multiple phenotypes. There is still an unmet need to characterize and understand underlying mechanisms taking place in the lungs in order to propose the most suitable therapeutic strategies for SA. For this purpose, we aimed to identify a local signature of severe asthma by conducting comprehensive multi-omics analysis of bronchoalveolar lavages fluids (BALs) from children with SA *versus* non-asthmatic (NA) controls.

Method. BALs were collected from twenty children with SA and from ten age-matched NA. We previously analyzed soluble and cellular immune components in those samples, and now propose to perform comprehensive analysis of their microbiota and their metabolome. Briefly, DNA from BALs was extracted and 16S rRNA gene (V3-V4 region) was amplified by PCR and sequenced. In parallel, untargeted metabolomics was performed using liquid chromatography coupled to high resolution mass spectrometry (LC-HRMS) following an established workflow for sample preparation, data acquisition and treatment. Each microbiome and metabolome dataset was first analysed independently by unsupervised multivariate analyses (Principal component analyses, PCA). Differences between groups for microbiota diversity indices, the relative distribution of each phyla and genera were then analysed. Metabolite set enrichment analysis (MSEA) and univariate supervised analysis were also performed. To identify a local signature of severe asthma, microbiota and metabolome data were further integrated, together with immune and with clinical data, using unsupervised Multi-Omics Factor Analysis (MOFA).

Results. Microbiota diversity was higher in children with SA *versus* NA, with higher relative abundances of *Streptococcus*, *Corynebacterium*, *Tropheryma whipplei*, *Dolosigranulum pigrum* and *Moraxella nonliquefaciens*. We identified 88 metabolites in BALs, but unsupervised PCA of corresponding data did not differentiate children with SA from NA. However, MSEA evidenced that biotin and carnitine synthesis, lysine degradation, methionine metabolism and spermidine and spermine biosynthesis pathways were significantly enriched in children with SA. Finally, multiblocks data integration identified a signature of SA, mainly described by metabolites and cytokines.

Conclusion. By integrating metabolome, microbiome and cytokines data obtained on BALs from children with severe asthma *versus* NA, our study uniquely described a local signature of SA.

1. Introduction

Asthma is characterized by chronic inflammation of the airways causing hyperresponsiveness to environmental exposures or viral infections [1]. Severe asthma (SA) is defined as uncontrolled asthma, i.e. occurrence of exacerbations despite high doses of inhaled corticosteroids (ICS) associated with second controllers, and despite correct use of medication and removal of modifiable and environmental factors such as tobacco exposure [2]. To compensate this poor response to treatment in SA patients, the last few years have seen the emergence of biotherapies. However, in order to propose them, it is necessary to know the phenotype of the disease, i.e. observable characteristics that result from a combination of

hereditary and environmental influences [3, 4], but also the underlying endotypes, i.e. distinct pathophysiologic mechanisms at cellular and molecular levels. The most well established classification of SA is the T2-high (eosinophilic) and T2-low (non-eosinophilic) endotypes [4, 5]. However recent studies have described the presence of several other cell types and markers of T1, T2, and/or T17 inflammation locally, underlying immune mechanisms far beyond a simplistic T2 paradigm [6–8]. Thus, the development of treatments adapted to each patient (precision medicine) needs a deeper description of endotypes and identification of associated biomarkers.

To date, biomarkers indicative of T2-high asthma include mainly fractional exhaled nitric oxide (FeNO), serum levels of periostin, and blood or sputum eosinophils [4, 5, 9]. Recently, we also showed that a large set of immune variables in blood and bronchoalveolar lavages (BALs) may differentiate children with SA form control subjects [6] and, among children with SA, frequent exacerbators from non-frequent exacerbators [10]. Adult patients with SA has also been associated with changes in the concentrations of some plasma metabolites, notably decreased levels of 1-stearoyl glycerol sulfate, dehydroisoandrosterone sulfate and androsterone sulfate and increased levels of oleoylethanolamide, sphingosine-1-phosphate, N-palmitoltaurine, 22-hydroxycholesterol and xanthine [11]. Another study of exhaled breath condensate (EBC) in adults, highlighted the contribution of amino acids (lysine) and lipids (eicosanoids, phospholipids and unsaturated fatty acids) metabolism in asthma severity [12]. To date, metabolomic studies of childhood asthma have been mainly performed on blood, urine, and exhaled breath condensate samples. A study performed in BALs indicated that children with persistent wheezing had higher abundances of choline, oleamide, nepetalactam, butyrylcarnitine, l-palmitoylcarnitine, palmitoylethanolamide, and various phosphatidylcholines [13].

The lung microbiota gradually develops after birth. Indeed, a study has detected viable bacteria in the lungs of mice as early as 3 days after birth, which increased slightly the first two weeks [14]. Its composition is influenced by physiological changes and exposure to environmental factors [15] and although it has not been as deeply investigated as the gut microbiota, studies have shown that microorganisms in the respiratory tract finely influence the local immune system and its regulation, epithelial barrier fonction (mucus production, epithelial cell permeability) and alveolarisation [16]. Imbalance between the symbiotic and pathological bacterial strains in the lung may then lead to altered immune development and inappropriate inflammatory responses [17]. The lungs of a healthy adult are colonised mainly by two phyla, *Bacteroidetes* and *Firmicutes* [18]. Several studies have shown that the airway microbiome of asthmatics differs from that of healthy adult subjects, with increased relative abundance of certain genera such as *Haemophilus*, *Neisseria*, *Moraxella*, *Staphylococcus*, and *Streptococcus* [19, 20] and interestingly, the composition of the respiratory microbiota seems to be linked to phenotypic characteristics of asthma [21]. However, whether the dysbiosis encountered in asthmatic patients is the cause or the consequence of the disease is not elucidated and microbiota composition appears to be influenced by treatments. A systematic review from Hartmann et al. [22] reported that corticosteroids may alter the composition of the respiratory microbiome and another study found that asthmatic patients had an increased abundance of *Ascomycota*, and a lower abundance of *Basidiomycota*, after 3 months of inhaled corticosteroid (ICS) treatment [23].

To improve our understanding of the pathogenesis of SA and go further into precision medicine, we used an integrated approach combining the description of phenotype (asthma symptoms, atopy, and lung function) with immune components (innate and adaptive immunity), metabolome, and microbiota composition in BAL samples. Multiblocks data integration of metabolites intensities, microbiota composition and cytokines concentrations assayed in BALs, allowed to describe a signature of SA in children, which the main contributors were cytokines and metabolites.

2. Material and methods

2.1. Patients

Twenty children with severe asthma (SA) were included. All patients were mainly from the Paris region and they were followed regularly in the department of paediatric pulmonology and allergy of Necker Hospital (Paris, France). Ten children with chronic respiratory disorders other than asthma and requiring endoscopy were also recruited as age-matched disease-control subjects (thereafter-called non-asthmatic, NA). Clinical data, patient characteristics and ethical statements are described in our previous studies [6, 7, 10]. Children with SA used higher doses of ICS and had a higher post-bronchodilator Forced Expiratory Volume in 1 sec (FEV_1) over Forced Vital Capacity (FVC) ratio, and higher blood eosinophil counts than control.

2.2. Sample collections

Broncho-alveolar lavages were collected during endoscopy that was performed at least four weeks after an infection or asthma exacerbation. Lavages were recovered after injection of 3 mL/kg of body weight of NaCl 0.9%. The standard bronchoscopy procedure was followed for each patient.

Cytology, bacterial cultures, and immunofluorescence testing for common viruses were performed as part of the clinical assessments [6, 24]. Among children with SA, bacterial cultures were positive for five children (three for *Haemophilus influenzae*, one for *Streptococcus pyogenes*, and one for *Staphylococcus aureus*). In NA children's, bacterial cultures were positive for five children (three for *Haemophilus influenzae*, one for *Haemophilus influenzae* and *Moraxella catarrhalis*, and one for *Staphylococcus aureus*). Viruses were found in four SA children (two with rhinovirus, one with both adenovirus and parainfluenza virus, and one with respiratory syncytial virus) while only one NA children had positive virology (non SARS-CoV2 coronavirus).

Recovered lavages were kept on ice and transferred to the research lab within 3-4hrs. After centrifugation (400×*g*, 10 min, 4°C), bronchoalveolar lavage supernatants were collected (thereafter called BALs). Two BALs aliquots were transferred at -80°C until metabolomics and cytokines analyses. Remaining BALs were additionally centrifuged (14,000×*g*, 20 min, 4°C), and dry pellets were stored at -80°C until DNA extraction and 16S rRNA sequencing.

2.3. Bronchial airway microbiota analysis

DNA extraction from BALs. DNA was extracted in sterile conditions from dry pellets, using the QIAamp Power Fecal DNA kit following manufacturer's recommendations (Qiagen; Courtaboeuf, France). Briefly, chemical then mechanical (FastPrep-24™, 2 × 40 s, 4 m/s) lyses were performed. After centrifugation (3 min, 18000×g), and protein precipitation, the DNA was purified on spin filter columns. DNA was eluted with 2 × 50 µL of water. Two extraction blanks (no BALs) were prepared alongside other samples to evaluate the contaminants from reagents, consumables and surrounding environment. DNA quantity was assessed using Qubit^{TM} (INVITROGEN, Villebon-sur-Yvette, France). The DNA concentration values were between 0.164 and 174 ng/µL.

PCR amplification of 16S rRNA gene. For both samples and extraction blanks, the V3 and V4 hyper-variable regions of the 16S rRNA gene were amplified with a forward 43-nucleotide fusion primer (5' CTT TCC CTA CAC GAC GCT CTT CCG ATC TAC GGR AGG CAG CAG 3') and the 14-nt broad range bacterial primer 343 F, and a reverse 47-nucleotide fusion primer (5'GGA GTT CAG ACG TGT GCT CTT CCG ATC TTA CCA GGG TAT CTA ATC CT 3') [25]. The amplifications were carried out using the following PCR conditions: 1 cycle at 95°C for 10 min, followed by 40 cycles at 95°C for 15 s, and a finishing step at 60°C for 60 s, with MolTaq 16S DNA Polymerase (Molzym). Amplifications were checked by visualization on agarose gel, and PCR products were sent to the sequencing platform (@BRIDGe platform, INRAE, Jouy-en-Josas, http://abridge.inra.fr/). Preparation of purified DNA libraries and sequencing of amplicons were carried out using MiSeq Illumina technology (Illumina, USA). Sequencing was performed in two independent batches, including both internal controls and replicates of several samples. Data were merged after various internal checks and validations: PCoA and PERMANOVA were performed after combining both datasets to ensure there was no significant difference between batches.

Bioinformatic analysis of 16S rRNA. Sequencing quality was checked using MultiQC tools from Galaxy-migale platform (https://galaxy.migale.inra.fr/) [26]. Sequences were first analysed using the FROGS pipeline (version 3.2.2) to obtain the OTU (Operational Taxonomic Unit) abundance table [27]. This bioinformatic analysis included noise suppression and grouping of sequences into OTUs using SWARM (Aggregation distance clustering = 1), removal of chimeras using VSEARCH, OTUs filtering (cluster size > 5.10e5, remove contaminant from phiX databank), taxonomic affiliation for each OTU (Silva-Pintail 100 database) and affiliations filtering (Minimum coverage 80%). After performing these filtrations and suppressing the reads obtained in extraction blanks from the dataset, we obtained 1.73×10^6 sequences. The final OTU table contained 514 OTUs with taxonomic affiliation. The representativeness of the obtained sequences and the sequencing depth were checked by performing rarefaction curves. Only two samples showed a lower depth in sequencing (12,663 and 16,694 reads respectively), which was however considered sufficient for further analyses.

2.4. Metabolomic analysis

Sample preparation. In order to perform sample normalisation [28, 29], total protein concentration (Pierce™ BCA Protein Assay Kit, Thermo Fisher Scientific) of BALs was first assessed. Protein concentrations ranged between 0.051 to 1.011 mg/mL. Then, 500 µL of BALs were concentrated (SpeedVac™), and solubilized in ultrapure water to obtain a final concentration of 0.139 mg of total protein /mL. Proteins were then precipitated by adding 4 volume of MeOH / 1 volume of samples [30]. After 90 minutes of incubation on ice and centrifugation ($20,000 \times g$, 15 min, 4°C), the supernatants were collected and aliquoted. Quality control (QC) was prepared by pooling equivalent volumes of all samples. Finally, all the samples and QC were dried under nitrogen (RotorVap LV-Biotage, 30°C, 5 bars).

LC-HRMS Analysis. Dried pellets were resuspended in 108 µL of buffer, containing 95% water and 5% acetonitrile both containing 0.1% formic acid. QC and diluted QC (1/2, 1/4 and 1/8) were prepared in the same buffer. QC, diluted QC and 100 µL of each biological samples were spiked with 5 µL of a standard mixture (Supplementary Table 1), and 10 µL of the resulting samples were analysed by liquid chromatography coupled to high-resolution mass spectrometry (LC-HRMS). LC-HRMS was performed on an Ultimate 3000 chromatographic system coupled to a Q-Exactive mass spectrometer (Thermo Fisher Scientific, Courtaboeuf, France) fitted with an electrospray (ESI) source operating in the positive (ESI⁺) ionization mode. Ultra-high performance LC (UHPLC) separation was performed at 30°C using C18 column (Hypersil GOLD C18, 1.9 µm, 2.1 mm × 150 mm column, Thermo Fisher Scientific). Mobile phases were 100 % ultrapure H_2O (phase A) and 100 % acetonitrile (phase B), both containing 0.1 % formic acid. Chromatographic elution was achieved with a flow rate of 500 µL/min. After injection of 10 µL of sample, elution consisted of an isocratic step of 2 min at 5% phase B, followed by a linear gradient from 5 to 100% of phase B for the next 11 min. These proportions were kept constant for 12.5 min before returning to 5% B for 4.5 min. The column effluent was directly introduced into the electrospray source of the mass spectrometer. Source parameters were as follows: droplet evaporation temperature, 280°C; capillary voltage, 5 kV; sheath gas pressure and the auxiliary gas pressure, respectively at 60 and 10 arbitrary units with nitrogen gas; mass resolution power, 50,000 m/Δm; full width at half maximum (FWHM) at m/z 200, for singly charged ions; detection from m/z 85 to 1000.

Diluted QCs were analysed in triplicates at the beginning of the sequence, while non-diluted QCs were introduced every six randomised biological samples for data normalization/standardization purposes.

Raw data (.raw files) were manually inspected using the Qual-browser module of Xcalibur (version 4.1, Thermo Fisher Scientific) and then converted to .mzXML format using MSconvert ("ProteoWizard", version 3.0.21079). Data extraction was performed using "XCMS" R package deployed on the open-source web-based W4M platform (https://workflow4metabolomics.org/) [31]. The filtration of the variables as well as the quality metrics were carried out using the phenomis R package (version 1.0.2) [32]. Features generated from XCMS were filtered according to the following criteria: (i) correlation between QC dilution factors and areas of chromatographic peaks (> 0.7), (ii) coefficient of variation of chromatographic peak areas of QC samples (< 30 %), and (iii) ratio of chromatographic peak areas of biological to that of blank samples (> 3). Intensities were corrected for signal drift by fitting a locally quadratic (loess) regression model to the QC values. Initially, 25,698 variables were extracted with XCMS

package, and 2,972 variables were retained after filtering. Feature annotation was then performed along the 2,972 variables using an in-house spectral database based on chemical standards analysed under the same analytical conditions [30, 33]. To be annotated features had to match accurate measured mass, considering a ± 10 ppm tolerance, and measured retention time, considering a 45 secondes tolerance. Annotations were then confirmed by MS/MS analyses based on in-house database spectra, allowing the highest level of confidence (level 1 according to Metabolomic Standards Initiative) [23].

2.5. Local cytokines and immmunoglobulines

We analysed 76 immune soluble components in BALs for each individual (cytokines, antibodies). Method and results are described in [6, 10].

2.6. Statistical analysis of microbiota and metabolites datasets

Metabolome datasets were log10 transformed and the variables were centered to the mean and scaled to unit variance.

Metabolites and microbiota datasets were then first analysed independently, using multivatriate unsupervised methods. Principal component analysis (PCA) was used to identify potential outliers (none identified) and to construct principal components to explain the variability in the dataset ("ropls" R package). Hierarchical clustering was built using the Pearson's distance and Ward's linkage on both rows and columns with the R package "complexHeatmap" (version 2.14.0) [37]. Correlation analyses between demographic and clinical data and microbiota or metabolites variables were then calculated independently of the asthmatic status, using the Spearman correlation test. We considered demographic variables collected at recruitment (age, Body Mass Index (BMI), gender, rural *versus* urban lifestyle), variables participating in the definition of the asthmatic status (FEV_1, FEV_1/FVC, number of severe exacerbations in the past years, Asthma Control Test (ACT) score, ICS dose), and those assessed independently in hospital lab (bacteriology and virology). Correlation matrices were represented using the R package "Heatmaply" (version 1.4.2).

For microbiota, we also determined diversity indices and the relative distribution of each phylum and genus (and species, if possible) using Easy16S tool (https://shiny.migale.inrae.fr/app/easy16S). The α-diversity was analysed by calculating the Chao1 index (estimated community richness) on rarefied data (all samples were normalized to have the same number of reads). ANOVA was performed to compare the α-diversity between groups. Statistical differences between NA and SA groups for individual OTUs abundance were also tested using the Mann-Whitney test with Benjamini-Hochberg false discovery rate (FDR) correction for multiple testing.

OTUs were then combined by genus ("OTUtable" R package, version 1.1.2), allowing to sum into a single vector the abundances of OTUs within the same genus. This allowed avoiding redundancy and bias for the integration, due to repetition of the same genus with multiple affiliations. The 514 OTUs (see results) were grouped in 119 final genera. Microbiota dataset were transformed using Centered Log Ratio transformation (CLR, "mixOmics" R package, version 6.22.0)

In parallel, Metabolite set enrichment analysis (MSEA) was performed on the peak intensity table of annotated metabolites using KEGG ID and MetaboAnalyst 5.0 [35], and using the Small Molecule Pathway Database (SMPDB, version 2.0) as a metabolite set library. The pathways with an adjusted p-value (FDR correction) less than 0.1 were selected. Statistical differences between NA and SA groups for metabolites involved in enriched pathways were investigated using the Mann-Whitney test on non-transformed data. Correlations between clinical data and metabolites were carried out as described for microbiota data. Supervised OPLS-DA analysis was computed in R ("ropls" package, version 1.30.0 [36]).

Immune datasets were log10 transformed and the variables were centered to the mean and scaled to unit variance

2.7. Multiblock data integration.

The three different datasets obtained from the same patients were then integrated together: 119 OTUs at genus level, 88 metabolites and 76 cytokines and immmunoglobulines from microbiota, metabolome and immune dataset, respectiveley. Integration was performed for all patients with no missing values in the different data set (NA = 30, SA = 20) The integrative analyses of these datasets in multi-blocks was performed using Multi-Omics Factor Analysis (MOFA) implemented in R ("MOFA2", version 1.8.0) [37, 38] to identify variations that are shared across multiple datasets and those that are supported by only one. Each variable from the three datasets participates to each factor construction, but with different weight scores. Features with no association with the corresponding factor are expected to have absolute weight values close to zero, whereas features with strongest association with the Factor are expected to have larger absolute weight values.

3. Results

3.1. Children with SA have higher microbial diversity and increased relative abundance of some bacteria in BALs

Whatever the asthmatic status, taxonomic analysis first showed that most of the OTUs detected in BALs were associated with *Firmicutes* (new name: *Bacillota*) phylum (34.28%), then *Proteobacteria* (or *Pseudomonadota*) (24.09%), *Bacteroidota* (20.88%) and *Actinobacteriota* (*Actinomycetota*) (14.82%) (Supplementary figure 1).

We then visualized microbiota composition of BALs using unsupervised methods (i.e. PCA) that we just coloured depending on the asthmatic status (Figure 2A). Microbial composition of BALs from control subjects appeared to be more homogeneous than that of children with SA, but no visible distinction between the two groups of children was evidenced (i.e. centroids overlapped), whatever the ACP component considered (Figure 2A and not shown). Unsupervised ascendant hierarchical clustering (AHC), gave comparable result (Figure 2B). Indeed, AHC identified four clusters of individuals, with one cluster containing most of the samples (i.e. 80% of control subjects and 85% of children with SA). It is worth noting that patients #14 and #15 (SA) formed a separate cluster, which is also the case for patient #1 (SA) and patients #12 and #27 (NA).

We then assessed the correlations between the bacterial genera identified in the BALs from all collected samples (independently of NA/SA status) and some demographic and clinical data (Figure 2). Abundance of *Kingella* genus was negatively and significantly correlated with age (r = -0.48) and that of *Lentimicrobium* (r = -0.48) with female gender. Female gender was also correlated with higher *Alloprevotella* (r = 0.49) and *Cantonella* (r = 0.51) relative abundances. *Treponema* (r = 0.47) was positively correlated to BMI and *Stomatobaculum* (r = 0.54) to rural lifestyle (Figure 1A). Significant negative correlations were observed between ICS dose and the abundances of *Marvinbryantia* (r = -0.48), *Kocuria* (r = -0.47) and *Coriobacteriales Incertae Sedis* (r = -0.47). ACT score was positively correlated to *Blautia* (r = 0.56) and negatively to *Pasteurellaceae* family (r = -0.58), whereas FEV_1/FVC negatively correlated to *Bacillus* (r = -0.46) and *Eikenella* (r = -0.60, Figure 1B).

We then analysed the relative abundances of bacterial taxa at the genus level from the 30 children included in our cohort (Figure 3A). We observed a strong heterogeneity within both children with SA and control subject children's, without evidencing any difference related to asthma (Figure 3A). Control subjects children #12 and #27 and SA child #1, already highlighted in HCA, showed very low diversity.

Despite the high heterogeneity and low number of individuals, the α-diversity (i.e. reflecting the number of different species observed in each sample) trended to be higher in children with SA than in control subjects (Figure 3B). Moreover, differential expression analysis evidenced nine genera/species that were significantly more abundant in BALs from SA than in that from control subjects (Volcano plot, Figure 4A). Indeed, BALs from children with SA had significantly more bacteria belonging to the genera *Streptococcus*, *Corynebacterium* and *Prevotella*, and to the species *Tropheryma whipplei*, *Dolosigranulum pigrum* and *Moraxella nonliquefaciens* (Figure 4B). Conversely, OTU corresponding to *Haemophilus* genus was drastically decreased in BALs from children with SA compared to controls (Figure 4B).

3.2. SA children have a specific BAL metabolome

We identified 88 metabolites in BALs, with the highest level of confidence (Supplementary Table 2). Annotated metabolites belonged mainly to amino acids/peptides, aromatic and aliphatic compounds and nucleosides/nucleotides analogues classes (Supplementary figure 2).

Unsupervised and colored PCA highlighted that annotated metabolome appeared more homogeneous in BALs from children with SA than in control subjects, but no visible distinction was observed between patient groups (Figure 5A). This was confirmed by non-supervised AHC, which identified two clusters of individuals, the first one containing most of the samples independently of the group (Figure 5B). The second cluster contained samples from three control subjects, including patients' number #12 and #27, i.e. for which BALs were already distinguishable by microbiota composition and diversity. No difference between the groups was observed on the other PCA axes (not shown).

Correlations between metabolites and the demographic data (Figure 6; independently of asthmatic status) evidencedthat a rural lifestyle was negatively associated to 5-aminovalerate (r = -0.51, Figure 6A), and that a positive bacteriology was positively correlated to adenine (r = 0.48) and glycine-N-prolyl (Pro-Gly, r = 0.57) and negatively correlated to phenylacetyl-L-glutamine (r = -0.52). For clinical data, we observed the dose of ICS positively correlated with the levels of benzocaine (r = 0.54), pyridoxal (r = 0.59), cotinine (r = 0.46), spermine (r = 0.50) and 5 methylthioadenosine (r = 0.54), and it was negatively associated with the levels of L-homoserine (r = -0.50), L-lysine (r = -0.54) and arginine (r = -0.55). Number of exacerbations positively correlated to spermine (r = 0.48). FEV_1/FVC was negatively correlated to N6-acetyl-L-lysine (r = -0.54, Figure 6B).

Despite the absence of a structuration depending on the asthmatic status, univariate analysis identified ten metabolites that were significantly increased in children with SA compared to control and 6 metabolites that were significantly decreased (Supplementary Figure 3), but differences did not remain after correction for multiple testing. Supervised analysis (OPLS-DA) did not allow defining a model that discriminated the two groups (not shown).

However, Metabolite Set Enrichment Analysis (MSEA) showed that pathways related to (i) biotin metabolism, (ii) carnitine synthesis, (iii) lysine degradation, (iv) methionine metabolism and (v) spermidine and spermine (also named polyamines) biosynthesis were significantly enriched in BALs from children with SA (Figure 6C and Supplementary Table 3). Within the biotin and carnitine synthesis and the lysine degradation pathways, we could only evidence a significant decrease of L-lysine levels in BALs from children with SA *vs* control subjects. Additionally, L-homoserine (methionine metabolism pathway) levels decreased in BALs from children with SA, whereas level of adenosine increased. Interestingly, this later pathway interacts with the polyamine biosynthesis pathway by enabling spermine and spermidine synthesis via S-adenosyl-methioninamine conversion into 5-methylthio-adenosine (Figure 6D and Supplementary Figure 4). Over the five metabolites belonging to the polyamines biosynthesis pathway, both spermidine and spermine levels were significantly increased in BALs children with SA compared to controls (Figure 6D).

3.3. Multiblock dataset integration evidenced that children with SA are discriminated from control subjects by combined metabolites and cytokines data

In a non-supervised framework, we performed a multi-omics factor analysis (MOFA) to obtain an integrative view of the covariations between multiple datasets assessed in BALs. The datasets considered were that of soluble immune factors (76 cytokines and total antibodies, see [6, 10]), and that of the 119 microbial genera and the 88 metabolites identified in the present study.

In this analysis, the 8 factors retained in the model were sufficient to reduce dimensions while explaining most of the global variance. This model explained up to ~48% of the variation in the metabolites dataset, ~50% of the variation in the immune dataset and ~26% of the variation in the microbiota dataset (Supplementary Figure 5A). The variance decomposition analysis calculated the percentage of variance explained by each factor and data modality. Factor1 and Factor2 captured a source of variability that was present across metabolites and immune modalities (Factor1: 27.71% and 22.24% for metabolites and cytokines, respectively, and Factor2: 12.64% and 4.01%, respectively). Factor3 and Factor5 captured a source of variation that was exclusive to the immune datasets (15.91% and 8.30%, respectively). Factor4, Factor7 and Factor8 captured variatons from microbiota data (15.59, 5.63% and 4.46% respectively, Supplementary Figure 5B). Pearson correlation was calculated between the eight factors. The highest correlations were observed between latent Factor1 and the Factors4, 6 and 7 (r = 0.46; 0.33 and 0.38 respectively). As expected, the correlations between Factors confirmed that each data modality provided different information, and allowed further analysis using this model (Supplementary Figure 5C).

Association between MOFA factors and clinical parameters was then investigated (Figure 7A). We observed that Factor1, mainly explained by the variance of immune components and metabolites, was significantly associated with severe asthma status, which was confirmed when projecting SA and NA patients separately on Factors 1 to 8 (Figure 7B). Indeed, Factor1 was evidenced as the only one that distinguished children with SA from control subjects. Factor 8, mainly explained by the variance of microbiota variables, correlated with a positive virology in BALs (Figure 7A). Other factors were not correlated to any of the clinical or demographic variables considered.

As Factor1 captured the variance associated with the severe asthmatic status (Figure 7B), and was mainly constructed by metabolites and cytokines variables, we went deeper to identify the metabolites and cytokines that mostly contributed to Factor1 and then that may participate in describing SA phenotypes. In the top 20 of features that contributed positively to the Factor1, we evidenced the cytokine APRIL (Figure 7C, Supplementary Figure 6) and the metabolites adenosine, guanosine, hypoxanthine and α-pinene-oxide (Figure 7C, Supplementary Figure 7). Conversely, the metabolites that contributed negatively to Factor1 were glycyl-L-leucine, N-acetyl-ornithine, N6-acetyl-L-lysine, L-alanyl-L-proline, lysine, L-prolyl-L-leucine (Pro-Leu), xanthosine, methionine, valyl-proline (Val-Pro), arginine, L-homoserine and phenylpyruvic acid (Figure 7C, Supplementary Figure 7). Cytokines that contributed negatively to Factor1 were IL-8, Matrix metalloproteinases 2 (MMP-2) and CCL20 (Figure 7C, Supplementary Figure 6).

Discussion

The objective of this study was to identify a signature of SA in BALs based on single-block and multi-block integration statistical analysis of microbiota, metabolome and immune datasets. Through this small but well-phenotyped cohort, we evidenced higher microbiota diversity and altered metabolic pathways and immune responses in SA children. Integration of all datasets highlighted that immune and metabolomics factors are the main contributors to the SA signature, when compared to NA.

First, we showed that SA children tend to have greater bacterial diversity than non-asthmatics. While there appears to be a consensus that a decreased alpha-diversity of the gut microbiome is linked to a declined health status, there is no clear evidence how this generalizes to the microbiomes of the lungs [39]. Moreover, some studies also revealed an increase in alpha diversity in the gut in epilepsy [40], autism spectrum disorders [41], or transient ischemic patients [42]. Then, we evidenced some genera/species that were more abundant in BALs from children with SA including *Streptococcus*, *Corynebacterium*, *Prevotella*, *Dolosigranulum pigrum*, *Moraxella nonliquefaciens*, and *Tropheryma whipplei*. Conversely, *Haemophilus* was less abundant in BALs from children with SA compared to control subjects. Other groups have shown that the airway microbiome of adult asthmatics had higher relative abundance of certain genera such as *Haemophilus*, *Neisseria*, *Moraxella*, *Staphylococcus*, and *Streptococcus* [19, 20]. Some studies rather confirmed that *Proteobacteria* (*Pseudomonadota*) phylum, particularly *Haemophilus spp.*, is more frequent in bronchial airway samples from adults and children with SA than in controls [19, 43, 44]. The control patients included in our study had various non-asthmatic pathologies including non-cystic fibrosis bronchiectasis, bronchopathy, and ciliary dyskinesia. Forty percent of these control subjects also had a positive bacteriology for *Haemophilus* (4/10), while only two out of 20 (10%) of children with SA had such a positive bacteriology. This may explain the discrepancy between our results and data published by other groups on the relative abundances of Haemophilus. *Actinobacteria* (*Actinomycetota*) or *Firmicutes* (*Bacillota*), mainly *Streptococci* have been found more prevalent in children with SA [20, 43, 45], which is consistent with our results. In addition to our results, others have shown that decreased abundance in *Corynebacterium* were associated with asthma exacerbations in asthmatic children [46] and that airway microbiota of children dominated by *Corynebacterium* and *Dolosigranulum* genera were associated with a lower risk of developing loss of asthma control [47]. This will be investigated in the follow-up of the children involved in our study. Hilty et al. [19], showed that *Staphylococcus spp.* were also present in excess in the airways of children with difficult asthma. However, we did not found any difference in the relative abundance of *Staphylococcus* between the two groups of children.

In parallel, a non-supervised analysis of the metabolome did not make it possible to distinguish between the two groups of children. Using grouped-based approach such as MSEA, we were able to highlight metabolic pathways enriched in children with SA, such as those of spermine and spermidine biosynthesis, also called the "polyamine biosynthesis pathway". In line with our results, increased levels of these metabolites were reported in the blood of adult asthmatics with active symptoms [48] and in lung tissue of ovalbumin (OVA)-sensitized and challenged mice, which are widely used as an animal model of asthma [49, 50]. Polyamines play important roles in cell survival and cell death pathways. For example, spermine was reported to promote eosinophils survival by inhibiting mitochondrial permeability

transition and repressing caspases activities [51]. In addition, the three polyamines spermine, spermidine and putrescine, have been shown to stimulate superoxide generation by neutrophils activated by fMLP (fMet-Leu-Phe) [52], which enhanced the surrounding oxidative stress and aggravated airway inflammation and bronchial hyperresponsiveness. Therefore, our study further supports the major role of polyamines in severe asthma. This is confirmed by the strong correlation between BALs levels of spermine and the number of exacerbations. The metabolites identified in our analysis are however entirely dependent on the database used. Our internal base allowing metabolite annotations contains a majority of endogenous metabolites: it is therefore more difficult to highlight altered bacterial metabolic pathways and / or correlation between metabolome and microbiota in our analysis.

To go deeper in the complexity of SA, we integrated BALs datasets for immune components (with cytokines and Ig variables previously described in [6, 7, 10]), microbiota and metabolome using a multi-omics factorial analysis with a non-supervised approach. The major sources of variations from the three datasets, comprising a total of 283 variables (distributed in 88 metabolites, 119 bacteria, 76 cytokines and Ig), were captured in eight latent factors. Interestingly, the first factor explained almost 50% of the total variance, and was strongly associated with SA. Main contributors of Factor1 were data from metabolites and immune datasets, whereas microbiota was a poor contributor. Furthermore, Factor4 captured the variance associated with microbiota variables and did not permit to distinguish the two groups. These results thus confirm the complexity of SA, but also the interest of combining different omics-datasets to obtain a local signature of this disease, as we recently observed in eosinophilic oesophagitis, a non-IgE mediated food allergy restricted to oesophagus [53].

In the present study, data integration evidenced that BALs from severe asthmatics were characterised by high concentrations of APRIL and CCL20 and by higher levels of metabolites from purine metabolism (guanosine, hypoxanthine and adenosine) and α-pinene-oxide. In accordance with our results, it was shown that the circulating levels of APRIL were significantly increased in patients with asthma compared with healthy normal controls [7, 36]. This cytokine then appears to be a consistent marker between BALs and blood. High concentrations of adenosine were already reported in BAL fluids from patients with asthma [55], and adenosine is known to cause bronchoconstriction when inhaled by asthmatic subjects [56]. Moreover, purine metabolism has been identified as being involved in asthma with higher levels of hypoxanthine in serum of asthmatic patients compared with healthy individuals [57]. However, in our study we did not find a strong correlation between parameters measured during spirometry tests (FEV_1, FVC), exacerbation number or ACT score and the metabolites belonging to this pathway.

With regards to the limited number of patients in this study, these results need to be confirmed on another independent cohort, with integration of other omic-dataset such as transcriptomic data that could indeed provided interesting information to refine asthma endotypes into intra-SA specific new groups [9].

In conclusion, thanks to a multi-omics approach, our study uniquely described composition of BALs collected from severe asthmatic children compared to non asthmatic. Our study provides new leads to understand the complex mechanisms involved locally in severe asthma. Such approach and results may

soon be used to identify new targets that will allow better diagnosis and treatment of children with severe asthma.

Abbreviations

ACT: Asthma Control Test; AHC: Ascendant Hierarchical Clustering; BAL: BronchoAlveolar Lavage; CV: coefficient of variation; EBC: Exhaled Breath Condensate; FA: Formic Acid; FeNO: Fractional Exhaled Nitric Oxide; FEV_1: Forced Expiratory Volume in the first second; FVC: Forced Vital Capacity; ICS: Inhaled CorticoSteroid; Ig: Immunoglobuline; MSEA: Metabolite Set Enrichment Analysis; MOFA: Multi-Omics Factor Analysis; NA: Non Asthmatic; OTU: Operation Taxonomic Unit; PCA: Principal Component Analysis; Pro-Gly: Glycine-N-prolyl; QC: Quality Controls; SA: Severe Asthmatic; UHPLC: Ultra-high performance liquid chromatographic

Declarations

Author Contributions

F.F, F.C, B.G, M.B: metabolomic extraction process development

M.G. & K.A.-P. sample processing & immune analysis

B.G, M.B: metabolomic data acquisition

A.B: PCR amplification of 16S rDNA

V.S.-C, M.B: microbiota data acquisition and treatment

E.V, C.H.-A, M.B: statistical analysis

K.A.-P, V.S.-C, M.B: writing—correction, review and editing

M.T, G.L, M.L.-M, K.A.-P: funding acquisition

All authors have read and agreed to the published version of the manuscript.

Acknowledgments

Fundings

Availability of data and materials

The datasets supporting the conclusions of this article are available in the data INRAE repository, BRIARD, Melanie, 2023, "Multi-omics analysis of bronchoalveolar lavages of children wih severe asthma", https://doi.org/10.57745/TTLZCF, Recherche Data Gouv, V1, UNF:6:Z1oENwpcuW/D/XOUs4xMvQ== [fileUNF].

Ethics Statement

The studies involving human participants were reviewed and approved by Comité de Protection des Personnes Ile de France 2. Written informed consent to participate in this study was provided by the participants' legal guardian/next of kin.

Conflict of Interest

The remaining authors declare that the research was conducted in the absence of any commercial or financial relationships that could be construed as a potential conflict of interest.

References

1. Global Initiative for Asthma. Global strategy fo asthma management and prevention. 2022.
2. Chung KF, Wenzel SE, Brozek JL, Bush A, Castro M, Sterk PJ, et al. International ERS/ATS guidelines on definition, evaluation and treatment of severe asthma. Eur Respir J. 2014;43:343–73.
3. Lezmi G, de Blic J. Assessment of airway inflammation and remodeling in children with severe asthma: The next challenge. Pediatr Pulmonol. 2018;53:1171–3.
4. Kuruvilla ME, Lee FE-H, Lee GB. Understanding Asthma Phenotypes, Endotypes, and Mechanisms of Disease. Clin Rev Allergy Immunol. 2019;56:219–33.
5. Haktanir Abul M, Phipatanakul W. Severe asthma in children: Evaluation and management. Allergol Int. 2019;68:150–7.

6. Adel-Patient K, Grauso M, Abou-Taam R, Guillon B, Dietrich C, Machavoine F, et al. A Comprehensive Analysis of Immune Constituents in Blood and Bronchoalveolar Lavage Allows Identification of an Immune Signature of Severe Asthma in Children. Front Immunol. 2021;12:700521.

7. Lezmi G, Abou-Taam R, Garcelon N, Dietrich C, Machavoine F, Delacourt C, et al. Evidence for a MAIT-17–high phenotype in children with severe asthma. J Allergy Clin Immunol. 2019;144:1714-1716.e6.

8. Wisniewski JA, Muehling LM, Eccles JD, Capaldo BJ, Agrawal R, Shirley D-A, et al. TH1 signatures are present in the lower airways of children with severe asthma, regardless of allergic status. J Allergy Clin Immunol. 2018;141:2048-2060.e13.

9. Ray A, Das J, Wenzel SE. Determining asthma endotypes and outcomes: Complementing existing clinical practice with modern machine learning. Cell Rep Med. 2022;3:100857.

10. Adel-Patient K, Grauso M, Abou-Taam R, Guillon B, Dietrich C, Machavoine F, et al. Immune signatures distinguish frequent from non-frequent exacerbators among children with severe asthma. Allergy. 2021;76:2261–4.

11. Reinke SN, Gallart-Ayala H, Gómez C, Checa A, Fauland A, Naz S, et al. Metabolomics analysis identifies different metabotypes of asthma severity. Eur Respir J. 2017;49:1601740.

12. Ntontsi P, Ntzoumanika V, Loukides S, Benaki D, Gkikas E, Mikros E, et al. EBC metabolomics for asthma severity. J Breath Res. 2020;14:036007.

13. Liang L, Hu M, Chen Y, Liu L, Wu L, Hang C, et al. Metabolomics of bronchoalveolar lavage in children with persistent wheezing. Respir Res. 2022;23:161.

14. Remot A, Descamps D, Noordine M-L, Boukadiri A, Mathieu E, Robert V, et al. Bacteria isolated from lung modulate asthma susceptibility in mice. ISME J. 2017;11:1061–74.

15. Saint-Criq V, Lugo-Villarino G, Thomas M. Dysbiosis, malnutrition and enhanced gut-lung axis contribute to age-related respiratory diseases. Ageing Res Rev. 2021;66:101235.

16. Mathieu E, Escribano-Vazquez U, Descamps D, Cherbuy C, Langella P, Riffault S, et al. Paradigms of Lung Microbiota Functions in Health and Disease, Particularly, in Asthma. Front Physiol. 2018;9:1168.

17. Barcik W, Boutin RCT, Sokolowska M, Finlay BB. The Role of Lung and Gut Microbiota in the Pathology of Asthma. Immunity. 2020;52:241–55.

18. Mathieu E, Marquant Q, Descamps D, Riffault S, Saint-Criq V, Thomas M. Le poumon est sensible aux effets locaux et à distance des microbiotes. Nutr Clin Métabolisme. 2021;35:242–52.

19. Hilty M, Burke C, Pedro H, Cardenas P, Bush A, Bossley C, et al. Disordered Microbial Communities in Asthmatic Airways. PLoS ONE. 2010;5:e8578.

20. Green BJ, Wiriyachaiporn S, Grainge C, Rogers GB, Kehagia V, Lau L, et al. Potentially Pathogenic Airway Bacteria and Neutrophilic Inflammation in Treatment Resistant Severe Asthma. PLoS ONE. 2014;9:e100645.

21. Taylor SL, Leong LEX, Choo JM, Wesselingh S, Yang IA, Upham JW, et al. Inflammatory phenotypes in patients with severe asthma are associated with distinct airway microbiology. J Allergy Clin

Immunol. 2018;141:94-103.e15.

22. Hartmann JE, Albrich WC, Dmitrijeva M, Kahlert CR. The Effects of Corticosteroids on the Respiratory Microbiome: A Systematic Review. Front Med. 2021;8:588584.

23. Huang C, Ni Y, Du W, Shi G. Effect of inhaled corticosteroids on microbiome and microbial correlations in asthma over a 9-month period. Clin Transl Sci. 2022;15:1723–36.

24. Lezmi G, Gosset P, Deschildre A, Abou-Taam R, Mahut B, Beydon N, et al. Airway Remodeling in Preschool Children with Severe Recurrent Wheeze. Am J Respir Crit Care Med. 2015;192:164–71.

25. Mata-Garrido J, Xiang Y, Chang-Marchand Y, Reisacher C, Ageron E, Guerrera IC, et al. The Heterochromatin protein 1 is a regulator in RNA splicing precision deficient in ulcerative colitis. Nat Commun. 2022;13:6834.

26. Ewels P, Magnusson M, Lundin S, Käller M. MultiQC: summarize analysis results for multiple tools and samples in a single report. Bioinformatics. 2016;32:3047–8.

27. Escudié F, Auer L, Bernard M, Mariadassou M, Cauquil L, Vidal K, et al. FROGS: Find, Rapidly, OTUs with Galaxy Solution. Bioinformatics. 2018;34:1287–94.

28. Jones KP, Edwards JH, Reynolds SP, Peters TJ, Davies BH. A comparison of albumin and urea as reference markers in bronchoalveolar lavage fluid from patients with interstitial lung disease. :5.

29. Ward C, Duddridge M, Fenwick J, Gardiner PV, Fleetwood A, Hendrick DJ, et al. Evaluation of albumin as a reference marker of dilution in bronchoalveolar lavage fluid from asthmatic and control subjects. Thorax. 1993;48:518–22.

30. Boudah S, Olivier M-F, Aros-Calt S, Oliveira L, Fenaille F, Tabet J-C, et al. Annotation of the human serum metabolome by coupling three liquid chromatography methods to high-resolution mass spectrometry. J Chromatogr B. 2014;966:34–47.

31. Smith CA, Want EJ, O'Maille G, Abagyan R, Siuzdak G. XCMS: Processing Mass Spectrometry Data for Metabolite Profiling Using Nonlinear Peak Alignment, Matching, and Identification. Anal Chem. 2006;78:779–87.

32. Imbert A, Rompais M, Selloum M, Castelli F, Mouton-Barbosa E, Brandolini-Bunlon M, et al. ProMetIS, deep phenotyping of mouse models by combined proteomics and metabolomics analysis. Sci Data. 2021;8:311.

33. Roux A, Xu Y, Heilier J-F, Olivier M-F, Ezan E, Tabet J-C, et al. Annotation of the Human Adult Urinary Metabolome and Metabolite Identification Using Ultra High Performance Liquid Chromatography Coupled to a Linear Quadrupole Ion Trap-Orbitrap Mass Spectrometer. Anal Chem. 2012;84:6429–37.

34. Sumner LW, Amberg A, Barrett D, Beale MH, Beger R, Daykin CA, et al. Proposed minimum reporting standards for chemical analysis: Chemical Analysis Working Group (CAWG) Metabolomics Standards Initiative (MSI). Metabolomics. 2007;3:211–21.

35. Pang Z, Zhou G, Ewald J, Chang L, Hacariz O, Basu N, et al. Using MetaboAnalyst 5.0 for LC−HRMS spectra processing, multi-omics integration and covariate adjustment of global metabolomics data. Nat Protoc. 2022;17:1735–61.

36. Thévenot EA, Roux A, Xu Y, Ezan E, Junot C. Analysis of the Human Adult Urinary Metabolome Variations with Age, Body Mass Index, and Gender by Implementing a Comprehensive Workflow for Univariate and OPLS Statistical Analyses. J Proteome Res. 2015;14:3322–35.

37. Argelaguet R, Arnol D, Bredikhin D, Deloro Y, Velten B, Marioni JC, et al. MOFA+: a statistical framework for comprehensive integration of multi-modal single-cell data. Genome Biol. 2020;21:111.

38. Argelaguet R, Velten B, Arnol D, Dietrich S, Zenz T, Marioni JC, et al. Multi-Omics Factor Analysis—a framework for unsupervised integration of multi-omics data sets. Mol Syst Biol. 2018;14.

39. Avalos-Fernandez M, Alin T, Métayer C, Thiébaut R, Enaud R, Delhaes L. The respiratory microbiota alpha-diversity in chronic lung diseases: first systematic review and meta-analysis. Respir Res. 2022;23:214.

40. Huang C, Li Y, Feng X, Li D, Li X, Ouyang Q, et al. Distinct Gut Microbiota Composition and Functional Category in Children With Cerebral Palsy and Epilepsy. Front Pediatr. 2019;7:394.

41. Coretti L, Paparo L, Riccio MP, Amato F, Cuomo M, Natale A, et al. Gut Microbiota Features in Young Children With Autism Spectrum Disorders. Front Microbiol. 2018;9:3146.

42. Yin J, Liao S-X, He Y, Wang S, Xia G-H, Liu F-T, et al. Dysbiosis of Gut Microbiota With Reduced Trimethylamine-N-Oxide Level in Patients With Large-Artery Atherosclerotic Stroke or Transient Ischemic Attack. J Am Heart Assoc. 2015;4.

43. Simpson JL, Daly J, Baines KJ, Yang IA, Upham JW, Reynolds PN, et al. Airway dysbiosis: *Haemophilus influenzae* and *Tropheryma* in poorly controlled asthma. Eur Respir J. 2016;47:792–800.

44. Zhang Q, Illing R, Hui CK, Downey K, Carr D, Stearn M, et al. Bacteria in sputum of stable severe asthma and increased airway wall thickness. Respir Res. 2012;13:35.

45. Chung KF. Potential Role of the Lung Microbiome in Shaping Asthma Phenotypes. Ann Am Thorac Soc. 2017;14 Supplement_5:S326–31.

46. McCauley K, Durack J, Valladares R, Fadrosh DW, Lin DL, Calatroni A, et al. Distinct nasal airway bacterial microbiotas differentially relate to exacerbation in pediatric patients with asthma. J Allergy Clin Immunol. 2019;144:1187–97.

47. Zhou Y, Jackson D, Bacharier LB, Mauger D, Boushey H, Castro M, et al. The upper-airway microbiota and loss of asthma control among asthmatic children. Nat Commun. 2019;10:5714.

48. Kurosawa M, Shimizu Y, Tsukagoshi H, Ueki M. Elevated levels of peripheral-blood, naturally occurring aliphatic polyamines in bronchial asthmatic patients with active symptoms. Allergy. 1992;47:638–43.

49. North ML, Grasemann H, Khanna N, Inman MD, Gauvreau GM, Scott JA. Increased Ornithine-Derived Polyamines Cause Airway Hyperresponsiveness in a Mouse Model of Asthma. Am J Respir Cell Mol Biol. 2013;48:694–702.

50. Jain V, Raina S, Gheware AP, Singh R, Rehman R, Negi V, et al. Reduction in polyamine catabolism leads to spermine-mediated airway epithelial injury and induces asthma features. Allergy. 2018;73:2033–45.

51. Ilmarinen P, Moilanen E, Erjefält JS, Kankaanranta H. The polyamine spermine promotes survival and activation of human eosinophils. J Allergy Clin Immunol. 2015;136:482-484.e11.

52. Guarnieri C, Georgountzos A, Caldarera I, Flamigni F, Ligabue A. Polyamines stimulate superoxide production in human neutrophils activated by N-fMet-Leu-Phe but not by phorbol myristate acetate. Biochim Biophys Acta BBA - Mol Cell Res. 1987;930:135–9.

53. Adel-Patient K, Campeotto F, Grauso M, Guillon B, Moroldo M, Venot E, et al. Assessment of local and systemic signature of eosinophilic esophagitis (EoE) in children through multi-omics approaches. Front Immunol. 2023;14:1108895.

54. Alturaiki W, Mubarak A, Mir SA, Afridi A, Premanathan M, Mickymaray S, et al. Plasma levels of BAFF and APRIL are elevated in patients with asthma in Saudi Arabia. Saudi J Biol Sci. 2021;28:7455–9.

55. Driver AG, Kukoly CA, Ali S, Mustafa SJ. Adenosine in Bronchoalveolar Lavage Fluid in Asthma. Am Rev Respir Dis. 1993;148:91–7.

56. Wilson CN, Nadeem A, Spina D, Brown R, Page CP, Mustafa SJ. Adenosine Receptors and Asthma. In: Wilson CN, Mustafa SJ, editors. Adenosine Receptors in Health and Disease. Berlin, Heidelberg: Springer Berlin Heidelberg; 2009. p. 329–62.

57. Ying L, Yan GX, Chun C, Xu Z, Juan W, Ting LT. Metabolomic Profiling Differences among Asthma, COPD, and Healthy Subjects: A LC-MS-based Metabolomic Analysis. Biomed Env Sci.
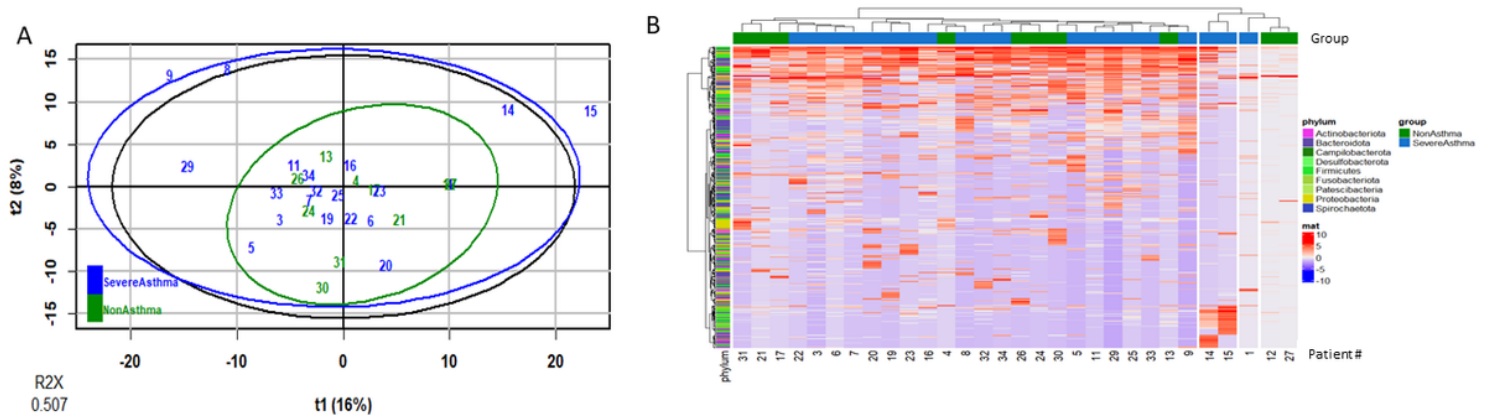
Figures

Figure 2

Figure 1

(A) **Graph of individuals on the two first dimensions of non-supervised PCA** constructed with OTU dataset, representing 24% of the total variance. 95% confidence ellipses based on Mahalanobis distance are represented in blue for SA data, and in green for NA data. Black circle correspond to correlation circle. **(B) Unsupervised ascendant hierarchical clustering** (AHC, Pearson correlation distance and Ward.D2 linkage). Columns represent individuals, with group indicated by colors (green: NA and blue: SA) and rows represent OTUs coloured by phylum.
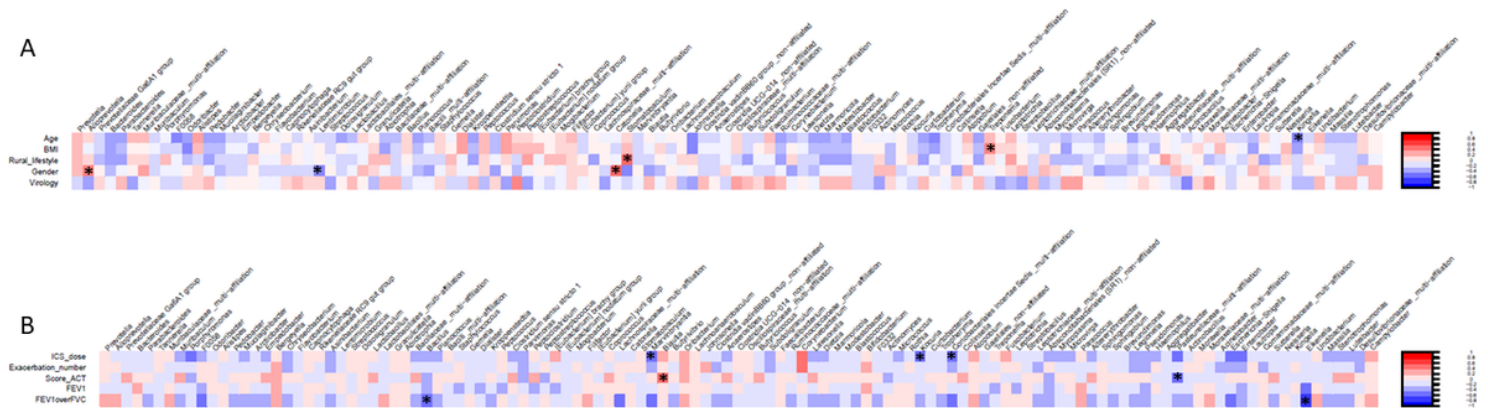

Figure 1

Figure 2

Correlogram representing correlation between genus abundances and (A) demographic data, (B) clinical data associated with asthma. ACT: Asthma Control Test; BMI: Body Mass Index; FEV$_1$: Forced Expiratory Volume in the first second; FVC: Forced Vital Capacity; ICS: Inhaled corticosteroid. *correspond to p value < 0.01.
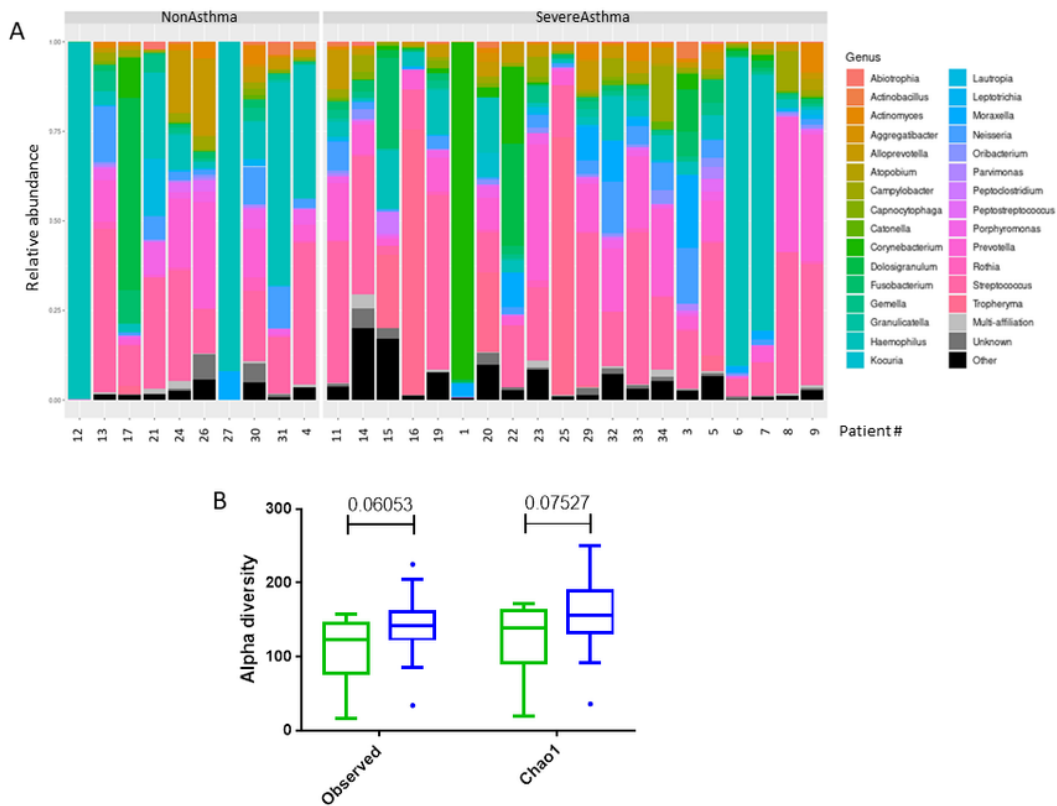
Figure 3

(A) **Stacked bar graph showing taxonomic composition** at the genus level for each individual sample, expressed as a proportion of total reads. Sample ID is on the x-axis. The top 30 genera with the highest average relative abundance are shown, and samples are stratified by asthma status. (B) **Box plots of microbiota alpha diversity values** distribution for both indices (Observed and Chao1 diversity) in BALs from non asthmatics (NA, green bars) and from the severe asthmatics (SA, blue bars) individuals. Outliers are shown as dots.
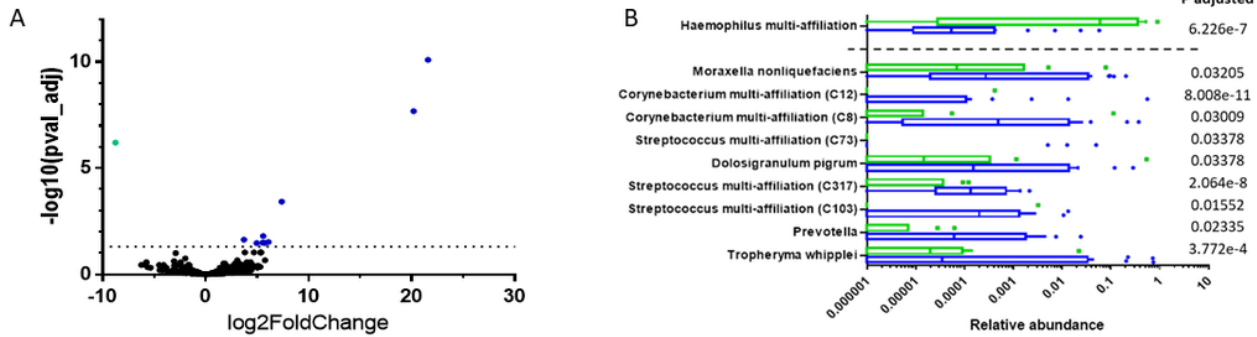
Figure 4

(A) Differential univariate analysis on the whole OTU dataset, presented by Volcano Plot for the comparison between SA and NA. Plot represents statistical significance (P-value) × magnitude of change (fold change). P-values were corrected with Benjamini-Hochberg (BH) method and considered significant for p< 0.05. Blue points correspond to OTUs significantly more abundant in BALs from SA than in NA, and green point OTUs significantly more abundant in BALs from NA than in SA. (B) Significantly different genera or species abundances in BALs from NA (green bars) and SA (blue bars) patients, represented as box plot. P-values were corrected with BH method.
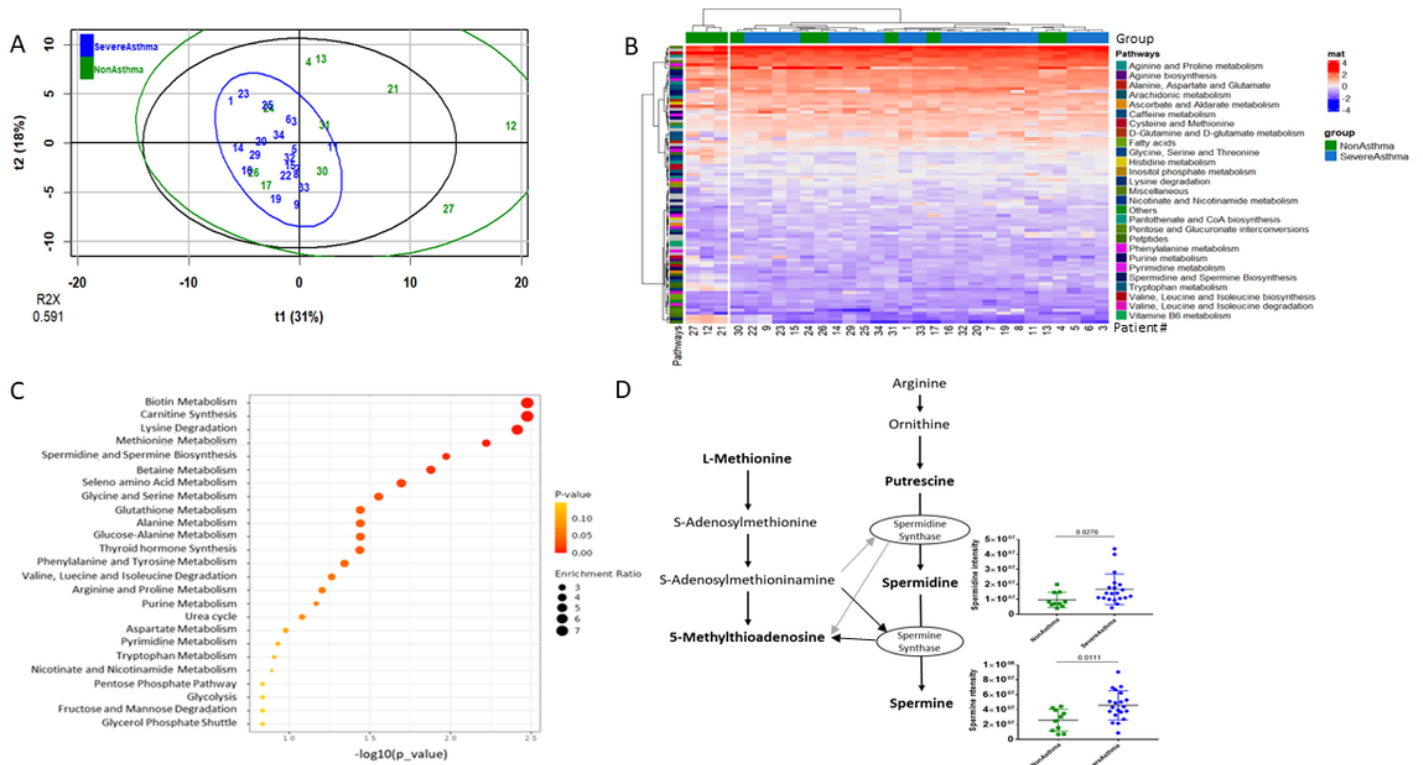
Figure 6

Figure 5

(A) Graph of individuals on the first two dimensions of non-supervised PCA constructed with all annotated metabolites dataset, representing 49% of the total variance. 95% confidence ellipses based on Mahalanobis distance are represented in blue for severe asthmatics data, and in green for non-asthmatics data. Black circle corresponds to correlation circle. **(B) Unsupervised AHC** (ascendant hierarchical clustering, Pearson correlation distance and Ward.D2 linkage). Columns represent individuals (green: non asthmatics; blue: severe asthmatics) and rows represent metabolites (coloured by metabolic pathways). **(C) Metabolite Set Enrichment Analysis results** (top 25) from the analysis of metabolites mapped in KEGG human metabolic pathways and signifcantly altered by severe asthma (Pathway enrichment analysis, MetaboAnalyst 5.0). The size of the circles per metabolite set represents the Enrichment Ratio and the color represents the p-value. **(D) Spermidine and spermine biosynthesis pathway.** Only metabolites in bold were annotated in our analysis. Comparison of metabolites intensity, involved in pathways, in non-asthmatic (green) and severe asthmatic (blue) patients. P-values were calculated with Mann-Whitney tests (no correction for multiple testing).
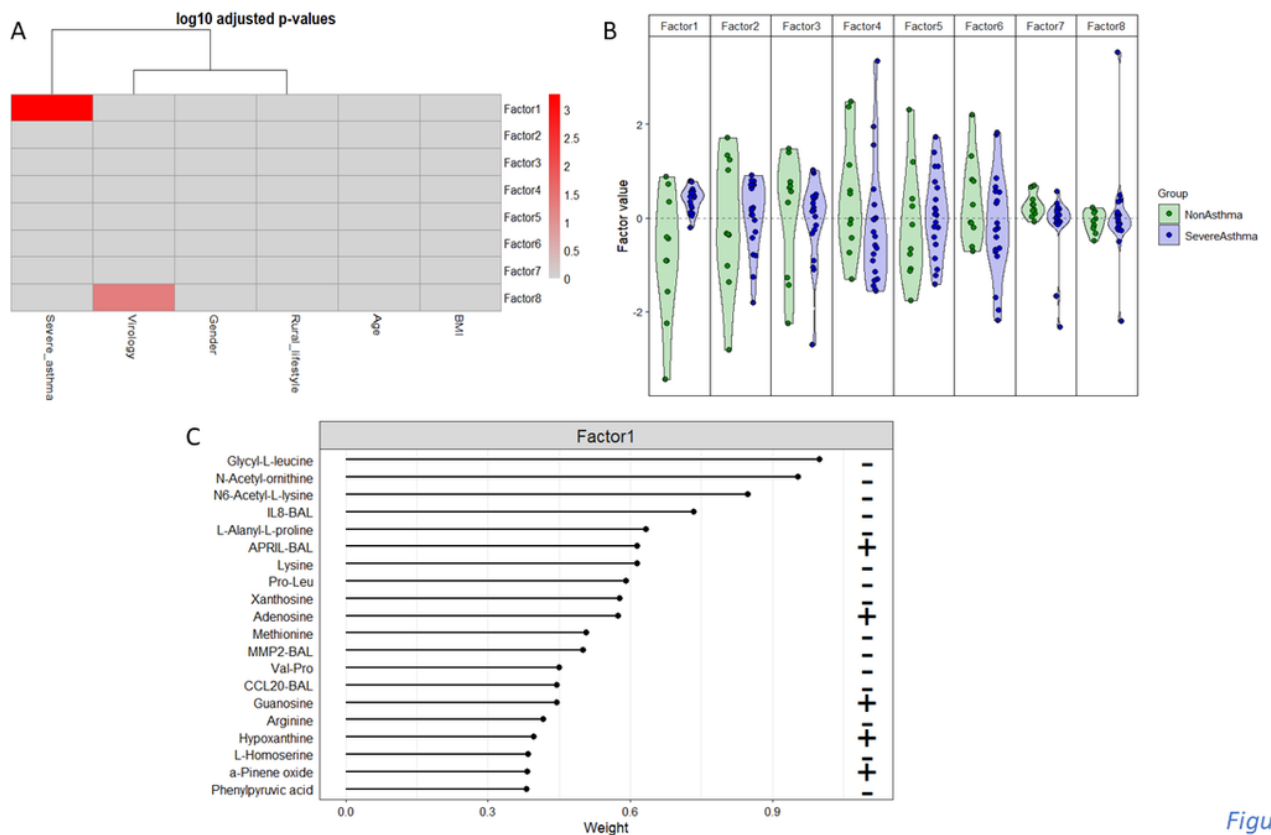
Figure 5

Figure 6

Correlogram representing correlation between metabolites intensities and (A) demographic data, (B) clinical data link to the pathology. ACT: Asthma Control Test; BMI: Body Mass Index; FEV$_1$: Forced Expiratory Volume in the first second; FVC: Forced Vital Capacity; ICS: Inhaled corticosteroid. *correspond to p value < 0.01.

Figure 7

Figure 7

(A) **Association of latent factors and clinical and demographic data**, latent factors identified with Multi-Omic Factor Analysis (MOFA). Only association with p-value adjusted <0.05 are represented. The color key bar indicates the log (p-value) of the correlation analysis. BMI: Body Mass Index. (B) **Values of the eight latent factors grouped and coloured by asthma pathology**. Green points represent non asthmatics and blue points severe asthmatics. As the data is centered prior to running MOFA, each Factor ordinates along a one-dimensional axis that is centered to zero. (C) **Absolute weights of the top 20 features** of Factor1. The weights provide a score for each feature on Factor1 construction. The sign of the weights indicates the direction of the effect. Features with no association with the corresponding factor are expected to have values close to zero, whereas features with strong association with the factor are expected to have higher absolute values, close to 1. A positive weight thus indicates that the feature has higher levels in the BALs of patients with positive factor values, and vice-versa. Pro-Leu: L-prolyl-L-leucine; Val-Pro: valyl-proline.

Supplementary Files

This is a list of supplementary files associated with this preprint. Click to download.

- Graphicalabstract.pptx
- Briardetal.SupplementaryTable1.xlsx
- Briardetal.SupplementaryTable2.xlsx

- Briardetal.SupplementaryTable3.xlsx
- Briardetal.SupplementaryFigurestitle.docx
- Supplementaryfigure1.png
- Supplementaryfigure2.png
- Supplementaryfigure3.png
- Supplementaryfigure4.png
- Supplementaryfigure5.png
- Supplementaryfigure6.png
- Supplementaryfigure7.png